HEDL-SA-2002 -FP

CONF-800609--12

MASTER

FRANK LOOP FORMATION IN IRRADIATED METALS IN RESPONSE TO APPLIED AND INTERNAL STRESSES

D. S. Gelles, F. A. Garner and H. R. Brager

April 1980

Paper to be presented at the ASTM 10th International Symposium on Effects of Radiation on Materials, to be held in Savannah, Georgia, June 3-5, 1980.

HANFORD ENGINEERING DEVELOPMENT LABORATORY
Operated by Westinghouse Hanford Company, a subsidiary of Westinghouse Electric Corporation, under the Department of Energy Contract No. DE-AC14-76FF02170

DISCLAIMER

FRANK LOOP FORMATION IN IRRADIATED METALS IN RESPONSE TO APPLIED AND INTERNAL STRESSES

D. S. Gelles, F. A. Garner and H. R. Brager

ABSTRACT

The Frank loop and dislocation microstructures developed in three face-centered cubic alloys during fast reactor irradiation have been examined to determine the influence of applied and internally-generated stress on loop evolution. It is shown that anisotropic stresses generate a corresponding anisotropy of Frank loop populations on the four close-packed planes. The loop populations thus represent a microstructural record of the irradiation creep processes in action. The ease of interpreting this record depends on the relative magnitudes of external and internal stresses.

Metals with low irradiation creep rates which also undergo concurrent and substantial phase changes during irradiation are subject to large and indeterminate levels of internally-generated stress which render the microstructural record uninterpretable with respect to the applied stress state. When the internally-generated stresses are small in comparison to the externally-applied stresses, a clear record of the SIPA* growth mechanism of irradiation creep is imprinted at low neutron fluences in the density and sizes of loops present on each set of close-packed planes. This record fades at higher fluences when the continued anisotropic formation, growth and unfaulting of Frank loops generates a corresponding anisotropy in the resultant free dislocation network, a process which alters the competition of sinks for point defects.

INTRODUCTION

In earlier reports it was shown that the evolution of Frank loops in AISI 316 was sensitive to the local stress state.[1,2] The stress state is not necessarily determined only by the external loading but is comprised of

---

* Stress-Induced-Preferential-Absorption of Interstitials.

additional internally-generated stresses which arise from the heterogeneity of swelling and phase changes as well as the dependence of irradiation creep on crystalline orientation and material texture. The externally-applied stresses in such experiments are usually constant and their magnitude is easily determined, while the internally-generated stresses are quite time-dependent and indeterminate.

If the Frank loops nucleate and grow in response to the local stress state, then the microstructural record comprising the loop population can be used to examine the action of various proposed irradiation creep mechanisms involving Frank loops. This has been successfully demonstrated in earlier studies[3,4] where the Frank loops formed in AISI 316 were shown to provide the first evidence that the stress-induced preferential absorption (SIPA) creep mechanism actually existed. The SIPA creep mechanism enables loops with favorable orientation to the stress state to have a larger preference for interstitial atoms than other loops with unfavorable orientation. SIPA is therefore a competitive growth mechanism.

The same evidence was used to relegate the stress-induced preferential loop nucleation to a lesser role. This conclusion was supported by Wolfer who evaluated the possibility that stress-assisted rotation of interstitial clusters might provide a method of preferential loop nucleation on planes favorably oriented to the applied stresses.[5] It was concluded that the rotation mechanism was not of sufficient magnitude to account for the partition of loops observed in the study of Okamoto and Harkness.[1]

As in most experimental studies, there were as many questions raised as were answered, and some of these second generation questions cast doubt on the validity of some portions of the original interpretation. In the following sections the earlier data are reviewed and assessed, and then recent data are presented which address the questions raised in the earlier study.

EXPERIMENTAL DETAILS

The specimens were irradiated in the form of thin-walled gas-pressurized tubes described in detail elsewhere.[2,6] These tubes were irradiated in

static sodium at elevated temperatures in the EBR-II Reactor. The irradiation vehicle is described in earlier reports.[6,7] Specimens 0.32 cm wide were cut from each pressurized tube by means of a slow-speed saw and a curved disk 0.3 cm in diameter was punched from each sample. Foil areas suitable for transmission electron microscopy were obtained using a Metalthin twin-jet electropolishing machine operating at 50 V with a 10% perchloric acid in acetic acid solution and a moderate pump speed. Transmission electron microscopy was performed on a JEM 200A microscope with a modified double-tilting specimen holder. Data analysis was performed using standard techniques based on stereoscopic measurements of foil thickness.

REVIEW OF EARLIER DATA

The first experimental evidence that Frank loops would be partitioned onto the four close-packed planes in an unequal manner[1] is shown in Figure 1. At the low fluence of 2.4×10^{21} n/cm^2, the loops that developed in this pressurized tube specimen have not yet experienced significant interaction. Voids were observed to coexist in the same region but their volume was not reported. It was not possible at that time to relate the loop distributions to the stress state. A stress-free specimen irradiated at comparable conditions was not available for comparison.

In a later effort[2] it was shown that the microstructure of two specimens irradiated under the same conditions but at different stress levels clearly demonstrated that stress played a large role in the deposition and growth of Frank loops on the various planes. As shown in Figure 2, the specimen without applied stress had essentially identical numbers and size distributions of loops on each close-packed plane. The specimen irradiated under stress exhibited a very large partition effect with nearly an order of magnitude difference in loop density between the least and most densely populated planes. The mean and maximum loop sizes of these two distributions were essentially the same, however, and it was proposed that the size distribution was controlled by two factors, one associated with the initial partitioning of loop formation on various planes and another associated with the annihilation of loops by intersection with the network dislocations. The network dislocations comprise about 95% of the total dislocation and loop line length of these specimens.

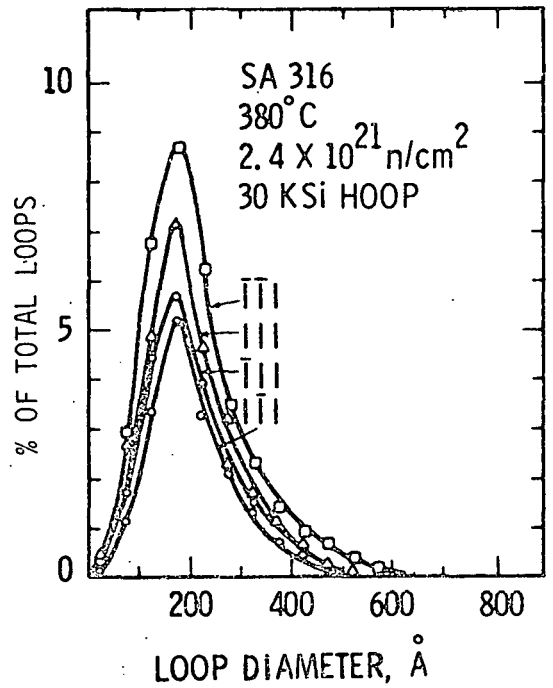

RELATIONSHIP TO BIAXIAL TENSILE STRESS STATE IS UNKNOWN

LOOP PLANE	ALIGNMENT FACTOR
$\bar{1}\bar{1}1$	1.30
111	1.07
$\bar{1}11$	0.86
$1\bar{1}1$	0.78

HEDL 8002-187.14

FIGURE 1. Frank Loop Distributions Observed at Low Fluence in Annealed SA 316 Irradiated Under a Biaxial Tensile Stress in a Pressurized Tube.(11)

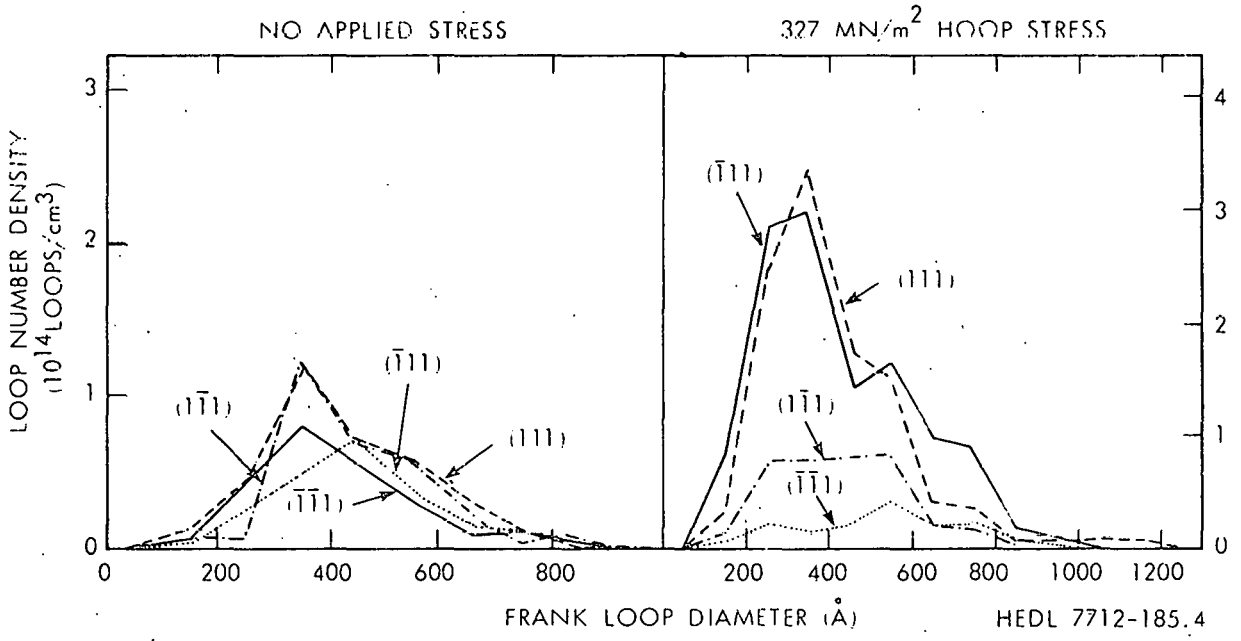

FIGURE 2. Comparison of Frank Loop Size Distributions on Each {111} Plane in Two Specimens of 20% Cold-Worked AISI 316 Irradiated at Different Stress Levels at 500°C to 3 x 10^{22} n/cm^2 (E >0.1 MeV).(2)

It is expected, however, that the mean size of the loop population will shift upward with fluence as the loops grow. And if stress enhanced their growth then the mean size should also increase with stress. As shown in Figure 3, this actually happens in solution annealed AISI 316 irradiated to a low fluence. Eventually in both annealed and cold-worked specimens, however, the network dislocation density saturates[8] and so does the loop size distribution.

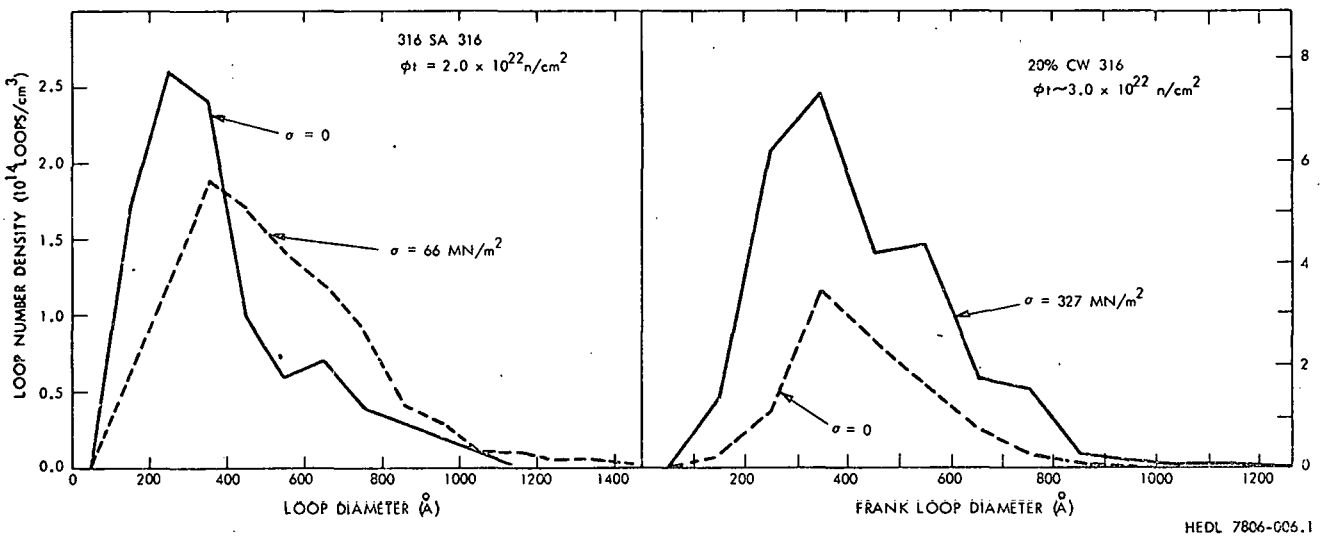

FIGURE 3. Comparison of Size and Frequency Data for Total Frank Loop Densities in Annealed and Cold-Worked Specimens Irradiated to Different Stress Levels.[2]

When the total density of loops on one plane is calculated, it exhibits a strong correlation with the normal component (σ_N) of the applied stress on that plane, as shown in Figure 4. Note that this correlation is observed in each of four specimens irradiated to different fluence levels and applied stresses. Even more importantly, however, when these data are plotted against the component of stress (σ_{DN}) involved in the description of the SIPA creep process, the data exhibit discernible trends with stress not only between planes within a specimen, but between specimens at different hydrostatic stress levels (σ_H) and fluence.[4] The stress component $\sigma_{DN} = (\sigma_N - \sigma_H)$ preserves the correlation with the normal stress component and allows that some planes with negative values of σ_{DN} will suffer a reduction in loop density.

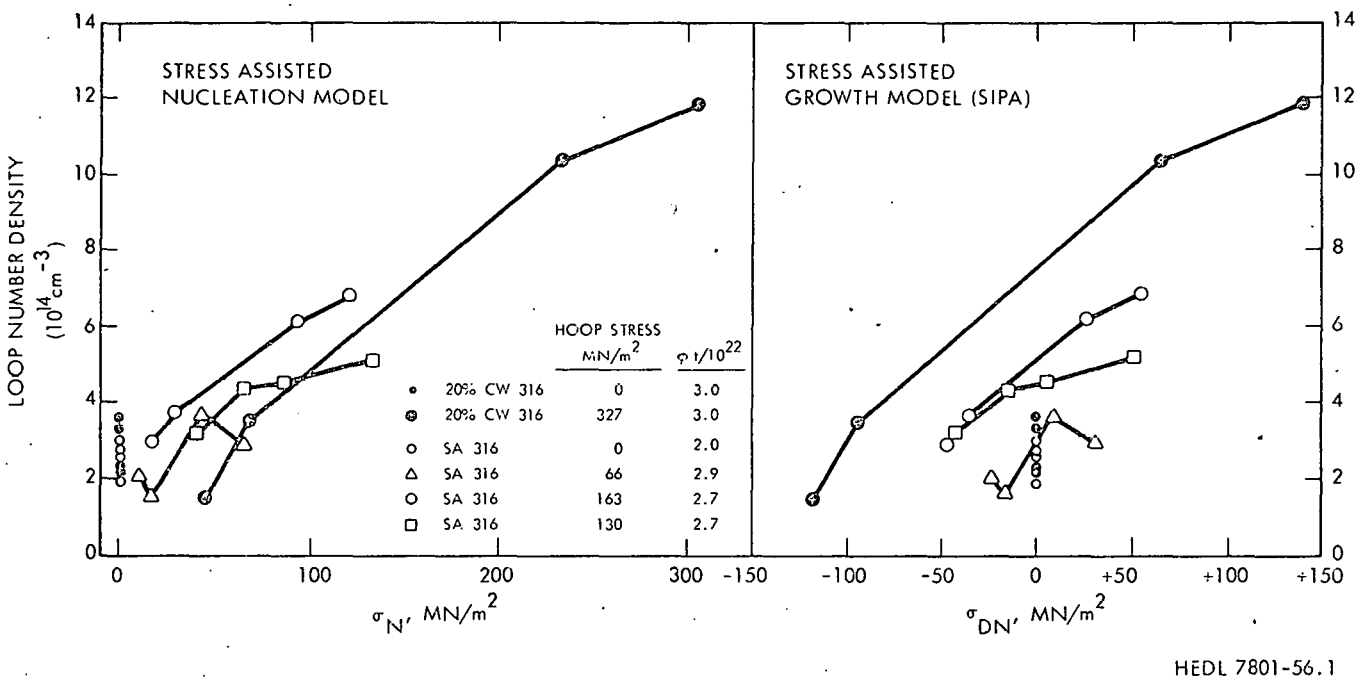

FIGURE 4. Comparison of Stress Affected Loop Population Data for AISI 316 in Light of Two Different Models.(4)

Although these data were judged to be reasonably conclusive experimental evidence of the operation of the SIPA creep mechanism on Frank loops, several questions persisted that detracted from the certainty with which this conclusion was stated. Since the specimens chosen for this study had either possessed initially or developed later a dislocation network as well as Frank loops, some important features of the SIPA-loop process may have been obscured. First of all, the SIPA process in itself cannot produce any increase in the total number of point defects which survive recombination and which are subsequently partitioned between the various microstructural sinks. As shown in Figure 3, this appears to be true in the annealed specimens since the total loop area was found to be roughly equal in both the stressed and unstressed specimens.(2) In the cold-worked specimens, however, there is a clear enhancement in the total loop area with stress. While SIPA operating on Frank loops alone cannot produce this result, it could generate an increase in loop area at the expense of the accompanying dislocation network since free dislocations are thought to have a lower bias for interstitials than that possessed by Frank loops.(9) Unfortunately, a free dislocation

does not impress in the microstructure a record of how far it has climbed and therefore the relative strain contributions of dislocations and loops cannot be determined.

If one were to design an experiment directed toward the observation of the SIPA mechanism operating on Frank loops, specimens would be chosen in which voids and loops were the only microstructural components, and in which the loops had not yet begun to interact. The loop size distribution would thus be determined by the SIPA process alone and not by intersection events. The void volume could also be used as an index of the partition of the Frenkel pairs. This was not possible in the earlier studies where the vacancies in voids outnumbered the interstitials in loops by a factor of roughly four in all specimens.[2] This indicated that the dislocation network was also a biased sink and that several generations of Frank loops may have already been unfaulted and added to the network.

Figure 4 also indicates that at zero or low applied stress levels, the loops were partitioned in an anisotropic manner but to a lesser extent. This observation has been interpreted as an indication of the internal stresses that exist in the material. The previously unpublished data shown in Figure 5(a) support this conclusion. Note that in the zero stress specimen the distributions at large sizes are essentially equal while at small sizes the distributions are different, particularly for one plane. It appears that nucleation is being retarded on that plane in the later stages of the irradiation but not earlier. The same trend can be observed in the specimen shown in Figure 5(b) where the externally applied stress is relatively low. Judicious choice of specimens could be used to address the possibility that internal stresses also play a role in the distribution of loops on the various close-packed planes.

Another question not addressed in the previous study was the long-term consequences of the anisotropy of loop nucleation. It was therefore decided to also examine specimens identical to those of the earlier study that were irradiated to higher fluences.

Recently, additional similar data have been obtained for AISI 316 and for two other alloys, Nimonic PE16 and Inconel 706. Comparison of these

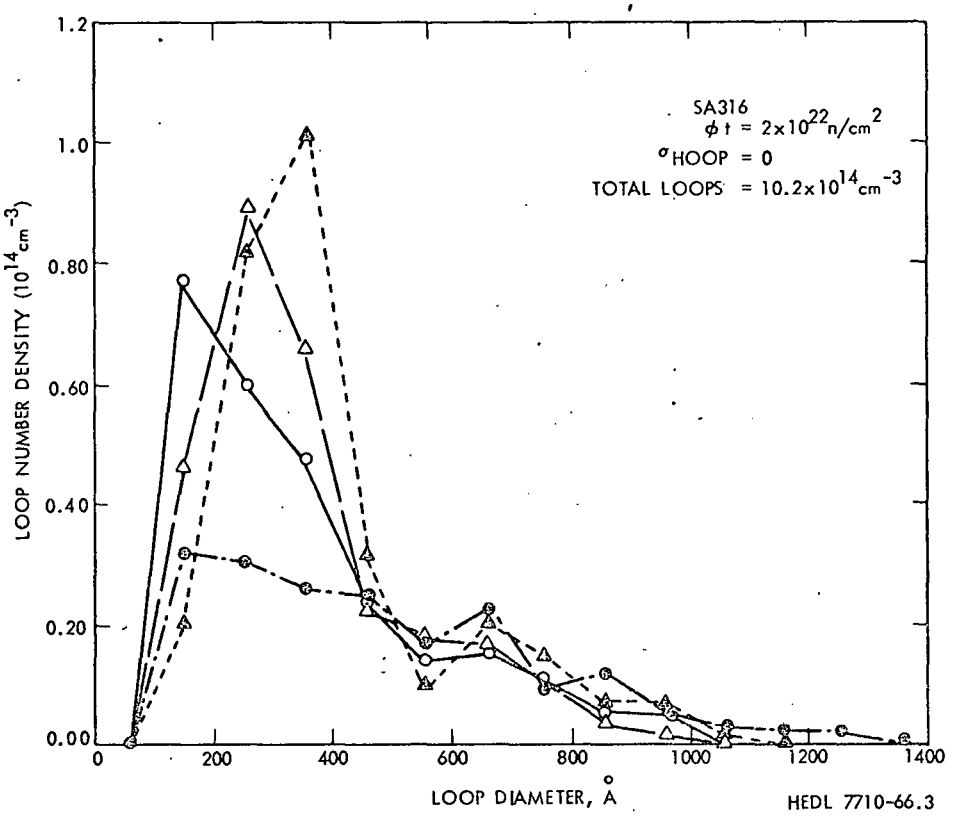

(a)

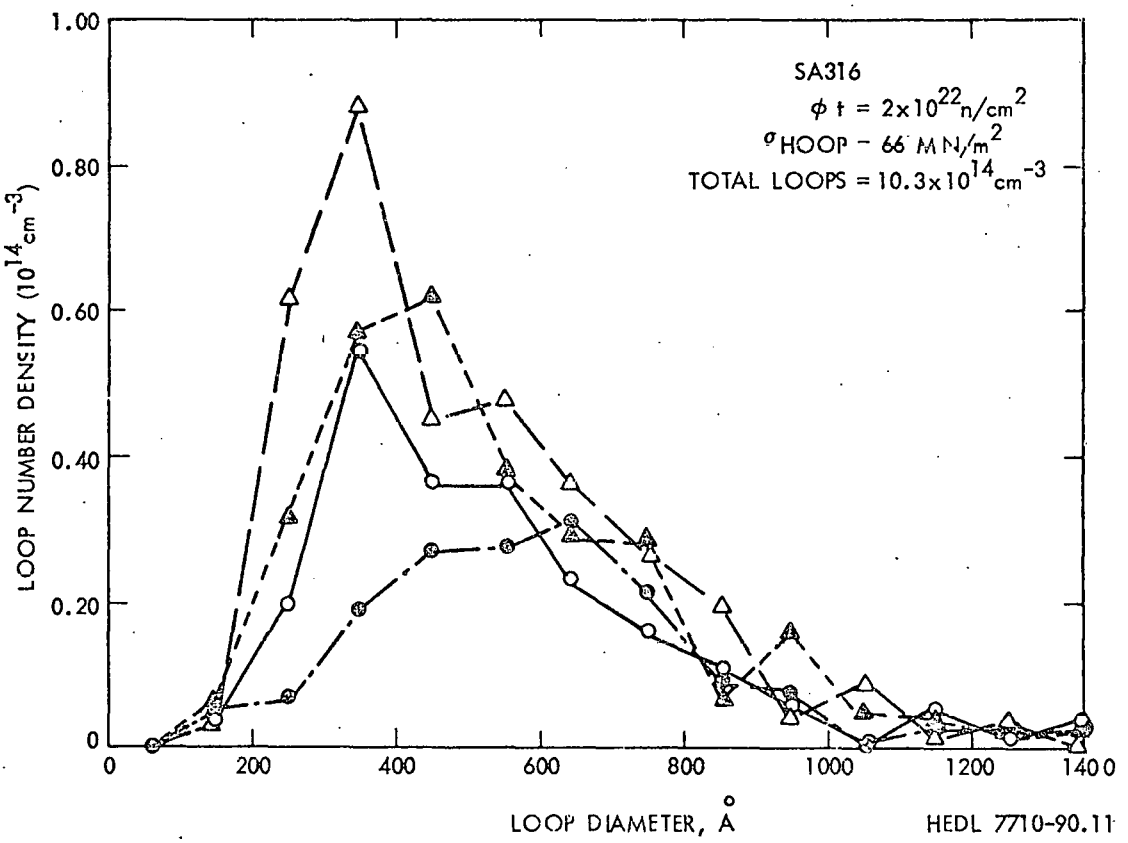

(b)

FIGURE 5. Frank Loop Distributions Observed on Each Plane of Annealed Specimens Shown in Figure 3.

with the earlier data has yielded significant new insight on the nature of the processes involved in loop growth and their contribution to deformation arising from irradiation creep. Whereas the data set on AISI 316 concerned a material in which the loop population quickly becomes a small and constantly regenerated part of the total dislocation microstructure, the new data sets involve materials in which Frank loops comprise essentially the entire dislocation microstructure developed throughout the irradiation. The loop populations in AISI 316 (particularly those in the cold-worked material) therefore contain only a record of recent loop growth, while the new data sets contain an integrated historical record of the entire loop population and its interaction with the instantaneous stress state.

Review and Analysis of Data on Nimonic PE16

This alloy was irradiated at 550°C to a fluence of 2.0×10^{22} n/cm^2 (E >0.1 MeV) in the solution-treated condition at two hoop stress levels, 0 and 167 MPa. As shown in Table 1, there was a measurable effect of the stress state on the bulk swelling, which increased from -0.6% (due to precipitate-related densification) at zero stress to +0.12% at 167 MPa. There was also some evidence of anisotropic densification in that the diameter changes were not obeying the expected simple relationship with density change. In other words,

$$\frac{\Delta D}{D} \neq \frac{1}{3} \frac{\Delta \rho}{\rho_0} . \qquad (1)$$

Figure 6 shows a comparison of the size distributions of Frank loops observed in each of the stressed and unstressed specimens. Table 2 contains the total loop density, stress and orientation data. Only regions which had not undergone loop unfaulting will be considered here. Additional loop populations from totally and partially unfaulted regions will be examined in future publications.

Several important observations can be drawn from the data of Figure 6 and Table 2:

(1) In the stress-free specimen the loop density and size distributions for sizes above 250 nm are essentially identical on all planes, while below

TABLE 1

COMPILATION OF DATA ON NIMONIC PE16 AND INCONEL 706 SPECIMENS IRRADIATED TO A FLUENCE OF 2 x 10^{22} n/cm^2 (E >0.1 MeV) AT 550°C

Material	Specimen Ident.	Stress Level (MPa)	$\frac{\% \Delta D}{D}$	$\frac{\% \Delta \rho^*}{\rho_o}$	$\frac{\% \Delta V}{V_o}$ (TEM)	Void Density (cm^{-3})	% Interstitial Atoms in Loops
ST PE16	AV69	0	-0.10	-0.60	0.06	1.2×10^{14}	0.051
ST PE16	AV75	167	-0.02	+0.12	0.08	1.7×10^{14}	0.059
STA 706	BP52	167	+0.05	-0.09	0.075† 0.060	3.1×10^{13}	0.023‡
ST 706	BA60	167	-0.11	-0.91	0.021† 0.025	1.1×10^{13}	0.021

* Overall densification is indicated by negative values.

† Two measurements were performed at different but adjacent areas.

‡ This value was measured in an area far removed from that where the void volume was measured.

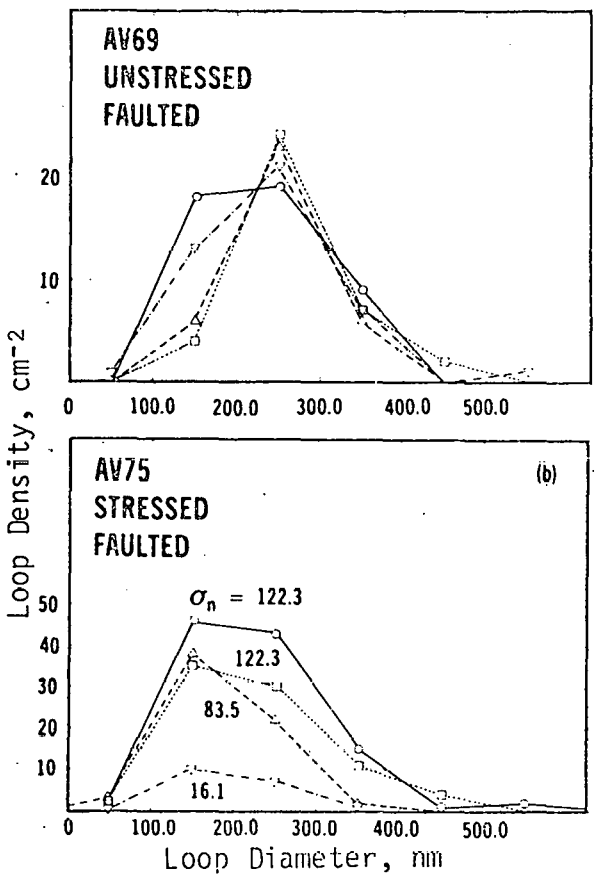

FIGURE 6. Frank Loop Size Distributions (Arbitrary Units) Observed in Unfaulted Regions of Solution-Treated Nimonic PE16 Irradiated to a Fluence of 2.0 x 10^{22} n/cm^2 (E >0.1 MeV) at 550°C, Hoop Stresses of 0 and 167 MPa. The normal stress levels for each plane are given in the figure.

TABLE 2

FRANK LOOP DATA FROM PRESSURIZED TUBES

Alloy	Specimen Ident.	Area Description	{111}	σ_n (MPa)	No. of Loops Counted	Loop Number Density (10^{12} cm^{-3})	Loop Mean Size (nm)	Loop Area (10^4 cm^{-1})
PE16	AV69	Unstressed/ Faulted		0	46	29	233	1.4
				0	35	22	251	1.1
				0	43	27	236	1.3
				0	37	23	270	1.4
					Total	101		5.1
PE16	AV75	Stressed/ Faulted	111	122.3	82	44	228	2.0
			$\bar{1}11$	16.1	18	9.6	194	0.31
			$1\bar{1}1$	83.5	65	35	188	1.04
			$11\bar{1}$	122.3	109	58	221	2.5
					Total	147		5.9
IN706	BA60	Stressed/ Faulted	111	27.0	55	480	45.5	0.87
			$\bar{1}11$	54.1	10	87	39.4	0.11
			$1\bar{1}1$	36.2	38	330	50.0	0.68
			$11\bar{1}$	26.9	42	360	47.1	0.66
					Total	1,260		2.3
IN706	BP52	Stressed/ Faulted	111	14.6	18	160	62.6	0.50
			$\bar{1}11$	96.9	28	240	58.3	0.70
			$1\bar{1}1$	148.8	25	220	51.1	0.47
			$11\bar{1}$	84.0	19	170	53.0	0.41
					Total	780		2.1

that size there are substantial variations in density. This indicates that some late-term effect is beginning to influence the growth rates of loops on different planes.

(2) The loops in this study are an order of magnitude larger than those reported in Reference 2 for AISI 316 at a comparable fluence. The number densities are correspondingly about an order of magnitude lower.

(3) The loop populations in the stressed specimen are altered substantially by the application of a biaxial tensile stress state. Not only is the loop population on one plane depressed below the stress-free level but the populations on the other planes are increased.

(4) A relationship exists between the total number of loops on any set of {111} planes and the magnitude of the normal stress component on that plane.

(5) While the total number of loops increases about one-half due to the application of stress, the loop area increases only 15%. An alternate interpretation is that within the accuracy of the measurements, the loop area probably remains constant. The mean loop size decreases accordingly to account for the difference in density.

Figure 7 shows the relationship between the total loop density (and area) on a given plane and the normal component of the deviatoric stress tensor, σ_{DN}, of the applied stress state for the stressed and unstressed specimens. (The values of σ_{DN} used here do not include any contributions from internally-generated stresses. The near-linear dependence of loop density on σ_{DN} in this alloy once again demonstrates the existence of the SIPA growth mechanism. Both the variation at zero stress and the deviations from linearity in the stressed specimen are once again thought to be due to the relatively minor effect of internal stresses in this alloy. This is surprising in light of the substantial densification (0.6%) that has occurred and indicates that the internal stresses involved probably were relatively short-lived.

Review and Analysis of Inconel 706 Data

No recognizable relationship could be found for the loop response to applied stress in either solution-treated or solution-treated and aged Inconel 706, both irradiated to a fluence of 2×10^{22} n/cm^2 (E >0.1 MeV) at 550°C under a hoop stress of 167 MPa (see Figure 8). Actually, as shown in Figure 9, the aged condition of the alloys shows some tendency toward a correlation of loop density with σ_{DN}. The lack of such a correlation is very obvious in the solution-treated condition, however. The Frank loops in the Inconel 706 specimens exist at densities comparable to those generated in AISI 316 at this fluence but no free network dislocations have yet been produced. Void swelling exists at quite low levels as indicated by the results of the microscopy measurements listed in Table 1.

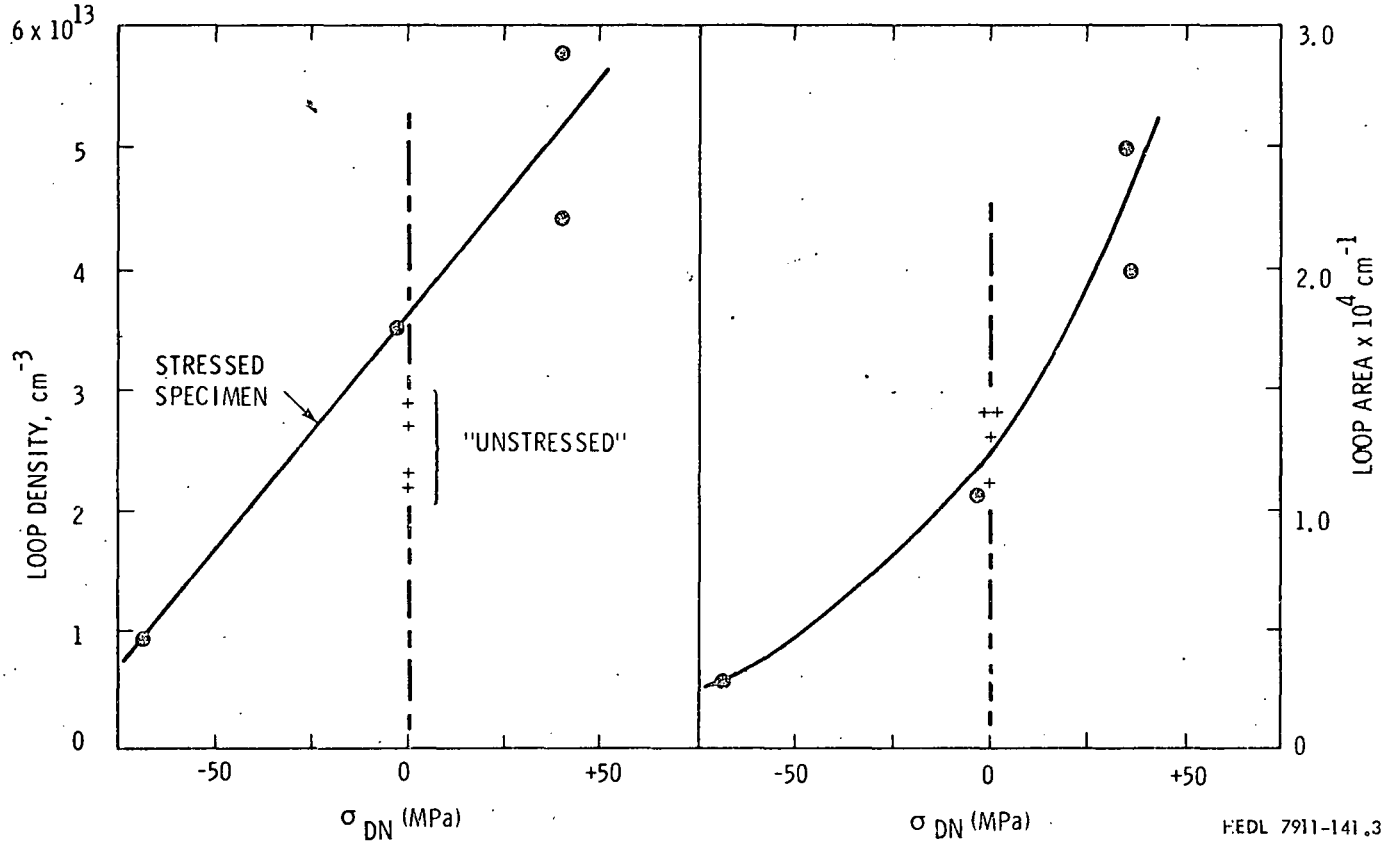

FIGURE 7. Correlation of Frank Loop Density and Area Versus σ_{DN} for Specimens Shown in Figure 6. Note that the increase in average loop area with stress is relatively small with applied stress.

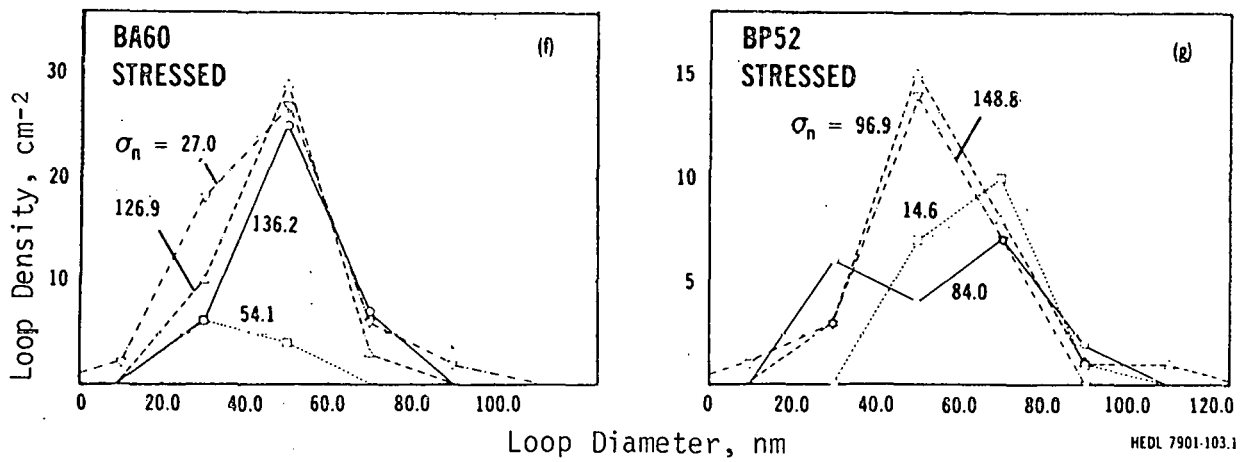

FIGURE 8. Frank Loop Size Distributions (Arbitrary Units) Observed in Specimens of Solution-Treated (BA60) and Solution-Treated and Aged Inconel 706 (BP52) Irradiated to a Fluence of 2.0×10^{22} n/cm^2 (E >0.1 MeV) at 550°C. Both specimens were derived from pressurized tubes subjected to a 167 MPa hoop stress.

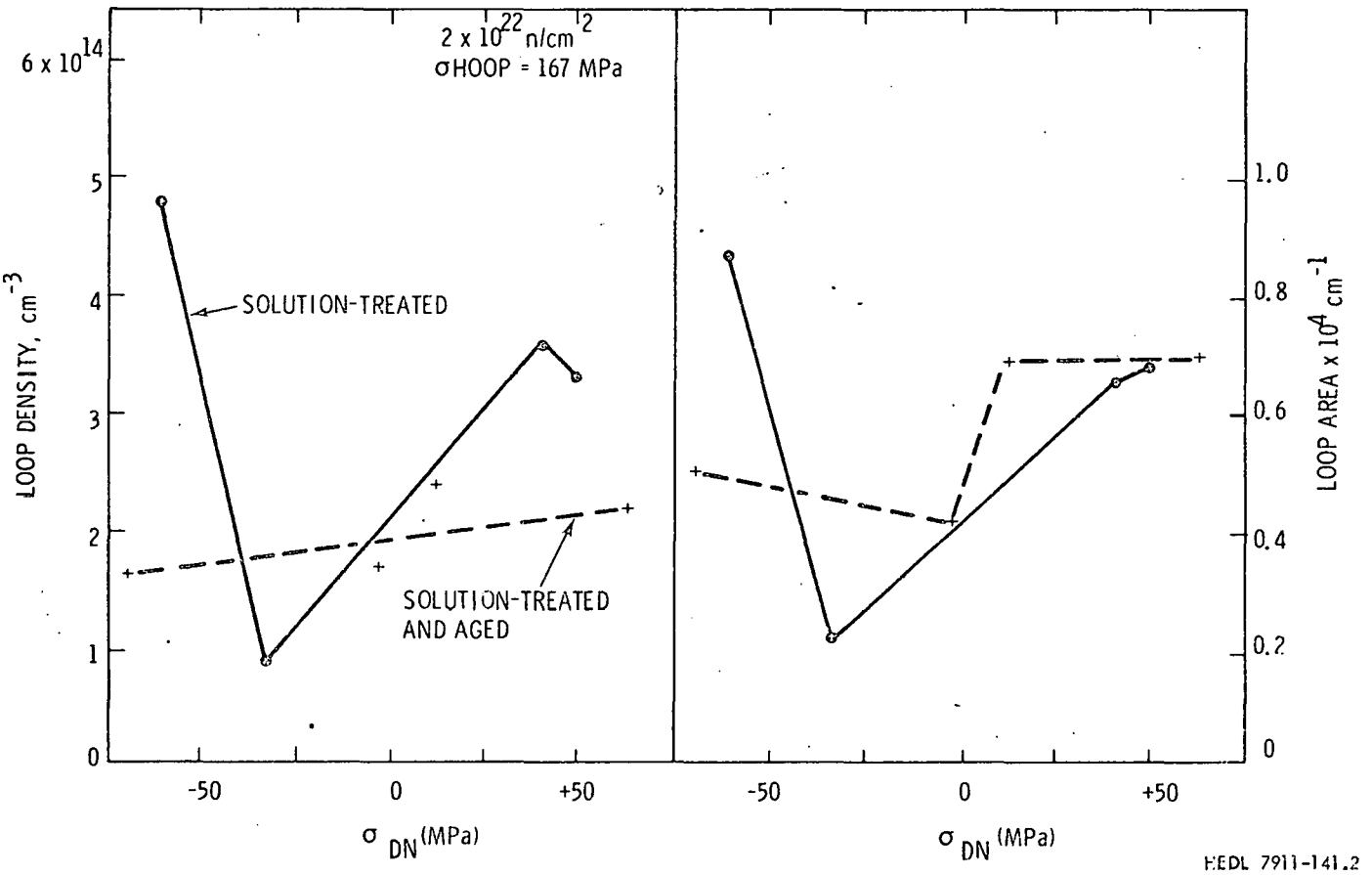

FIGURE 9. Loop Density and Area Versus σ_{DN} for Specimens Shown in Figure 8.

A possible clue to the lack of a relationship between the loops and the applied stress state can be found in the relative behavior of the aged and annealed specimens. The aged specimen underwent a substantial change in density during the aging process and then densified a smaller amount (about 0.1%) during irradiation. However, the solution-treated specimen underwent a radiation-induced densification of 0.91%. To reconcile the existence of a correlation with stress in the Nimonic PE16 data and a lack of a correlation in the annealed Inconel 706 data, it would be necessary to assert that the annealed Inconel 706 specimens were subjected to a more prolonged period of substantial internal stress than were the Nimonic PE16 specimens. Since the stress state is determined not only by the volume change and its anisotropy but also by the irradiation creep compliance, this appears to be a reasonable assumption. Inconel 706 is known to have very low rates of irradiation

creep,[7] a situation which would prolong the time required to relax the internal stresses. Even with sluggish rates of creep it would be expected that relaxation of the stresses arising from the much smaller level of volume change in the aged Inconel 706 would be much easier. Therefore some correlation of loop density and the externally-applied stress state might be expected.

Analysis of AISI 316 Data

The two specimens examined in this study were derived from the N-lot heat of 20% CW AISI 316 after irradiation at 475°C to a fluence of 9.3×10^{22} n/cm^2 (E >0.1 MeV) in the same subcapsule of the X-157C experiment. Specimen AN was not pressurized and specimen AP contained a gas pressure which generated a hoop stress of 30 ksi (207 MN/m^2).

Tables 3 and 4 contain a compilation of the microstructural data derived from the stressed and unstressed specimens. Voids have developed at this fluence in the heterogeneous manner usually observed in cold-worked steels. Therefore, to determine the effects of stress it is necessary to sample a number of typical areas to attain a representative average behavior for each specimen. Three or more areas were analyzed in each specimen and indicate that the effect of stress lies primarily in the enhanced nucleation of voids rather than in acceleration of their subsequent growth. This conclusion is in agreement with that obtained from lower fluence data on solution-annealed steel[2] and the Nimonic PE16 data shown in Table 1.

The dislocation density appears to be within the range observed earlier ($6 \pm 3 \times 10^{10}$ cm^{-2}) in fuel pin cladding.[8] This confirms the proposed saturation density concept of dislocation behavior in which the alloy matrix evolves toward a dislocation density that is relatively independent of neutron flux, irradiation temperature and alloy starting condition.[8]

Attempts to derive data on the Frank loop populations proved to be quite difficult due to the exceptionally complex nature of the microstructure and therefore yielded results which were below the original expectations of the experiment. It was hoped that the planar anisotropy of loop populations generated in response to internal and external stress fields would be as

TABLE 3

MICROSTRUCTURAL DATA FROM THE X-157C EXPERIMENT
(20% CW 316 AT 475°C AND 9.3 x 10^{22} n/cm^2, E >0.1 MeV)

	Specimen AN (Unstressed)	Specimen AP (30 ksi Hoop Stress)
Voids		
Void Volume (%)	1.67, 1.28, 1.02, 1.78	3.71, 3.61, 3.77
Void Density ($cm^{-3}/10^{15}$)	1.17, 0.97, 0.81, 0.99	1.58, 2.47, 1.26
Mean Diameter, nm	25.9, 35.6, 23.1, 27.5	30.4, 24.5, 33.8
γ' Precipitates		
Volume Fraction (%)	2.4	2.2
Precipitate Density (cm^{-3})	4.5 x 10^{15}	4.0 x 10^{15}
Mean Diameter, nm	16.5	17.0
Network Dislocations		
Density ($cm^{-2}/10^{10}$)	6.6, 8.0, 5.0	3.0
Density Change		
$-\Delta\rho/\rho_o$ (%)	1.7	2.8

TABLE 4

FRANK LOOP DATA* FROM THE X-157C EXPERIMENT
(20% CW 316 AT 475°C AND 9.3 x 10^{22} n/cm^2, E >0.1 MeV)

	Plane				
	I	II	III	IV	Volume Average
Specimen AN (Unstressed)					
Area #1	1.76 x 10^{14} 52.2 nm	2.16 x 10^{14} 49.3 nm		- -	7.8 x 10^{14} 50.8 nm
Area #2	1.12 x 10^{14} 45.7 nm	0.72 x 10^{14} 47.0 nm	0.54 x 10^{14} 41.3 nm	- -	3.2 x 10^{14} 44.6 nm
Area #3	1.42 x 10 48.3 nm	- -	- -	- -	5.7 x 10 48.3 nm
Specimen AP (Stressed)					
Area #4**	8.65 x 10^{13} 30.7 nm	6.83 x 10^{13} 28.3 nm	5.9 x 10^{13} 38.3 nm	- -	2.9 x 10^{14} 32.6 nm

* Numbers represent loop densities (cm^{-3}) and mean loop diameters.
** Only one area was analyzed.
\- Not determined for this plane.

measurable at this high fluence as it had been at lower fluences.[2] The loop densities and sizes shown in Table 4 thus represent the authors' best judgment of loop densities and are presented only for those (111) planes for which reasonably confident measurements could be obtained. The volume-averaged numbers on the right side of Table 4 assume that the unmeasured planes contain loop densities at the average density observed on the measured planes.

Several significant observations can be drawn from the loop data in spite of their shortcomings. In Area #2 of the unstressed specimen, a clear anisotropy of the loop distribution due to internal stress can be discerned. This variation in planar densities involves roughly a factor of two and is consistent with the results of lower fluence data. The total loop density in this and other areas of the unstressed specimens averages $5.6 \pm 2.3 \times 10^{14}$ cm^{-3}. This value is considerably less than the 1.14×10^{15} cm^{-3} observed at lower fluence, however, and indicates that loops are either being nucleated at lower rates at this fluence or annihilated faster. This latter process would lead not only to lower loop densities but also to smaller loop diameters. Since the 44.6 nm mean diameter found in Area #2 compares well with the 42.5 nm found at lower fluence,[2] the latter process does not appear to be dominant in determining the loop density. As shown in the next paragraph, the opposite conclusion is reached for the stressed specimen. Although the loop density has fallen it has not fallen far enough to convince the authors that the loop nucleation process has ceased, since calculations[10] indicate very short mean lifetimes for Frank loops.

When stress is applied to a specimen several significant features of the loop response are evident. Not only does the loop number density drop to about half that observed in the unstressed specimen but the mean loop diameter also decreases. This occurs in spite of the demonstrated tendency of applied tensile stresses to increase the total loop density in this alloy. It appears that the increased creep rate observed in this material at higher fluence has added an additional factor to the loop annihilation model. Whereas it was previously assumed that the loops grew fast enough to allow the network dislocation lattice to be considered as stationary, it now appears

that the loops will be annihilated by dislocation-loop intersection events at higher rates when the loop densities are relatively low and the average dislocation velocity increases with applied stress. A slight reduction of mean loop size with stress was also observed in the lower fluence experiment.

There is some anisotropy reflected in the loop size distribution of the stressed specimen but the level of anisotropy is consistent with that arising from internal stresses alone. It does not reflect the level of applied stress as had been anticipated based on the low fluence experiments. This result may reflect a fundamental change in the microstructural record left by irradiation creep at higher fluences.

DISCUSSION

The data indicate that at least at low fluences the Frank loop populations respond to anisotropy in the applied stress state in a manner which supports the existence of the SIPA creep mechanism. When there is no intervening or competing microstructure, the SIPA-induced partition of interstitial atoms is observed to operate in a manner which does not violate the principle of conservation of mass. In other words, there is no stress-assisted generation of additional interstitials. It is therefore safe to assume that the enhancement of loop area observed in 20% cold-worked AISI 316 arises from the stress-driven competition between loops and free dislocations for the available interstitials.

It is interesting to note that within experimental error, the number of vacancies in voids corresponds to the number of interstitials in loops for those Nimonic PE16 and Inconel 706 specimen areas for which both void and loop measurements were made (see Table 1). This is a further indication that no other microstructural components compete for the available defects.

It appears from the Inconel 706 data that the levels of internally-generated stress can be very large and can render the microstructural record uninterpretable with respect to the applied stress state. The largest levels of stress will arise in those alloys whose density change and creep properties are mismatched. Since swelling and creep tend to be matched in

their magnitudes, large internal stresses will arise only in those alloys with large precipitation-related density changes and low creep rates.

The AISI 316 data show that loop nucleation continues to high fluence even in network-dominated microstructures. The lack of a clear and large anisotropy of loop densities at high fluence implies that the SIPA process either declines with fluence or its microstructural record is suppressed. It is felt that both of these processes may be occurring.

First, remember that the SIPA record is contained in a measurable way in the loop population only, but that the dislocations also must respond to the SIPA process. Wolfer[5] notes that the net current of interstitials to a Frank loop is determined partially by the quantity $[(Z_I^S/Z_V^S) - (\bar{Z}_I/\bar{Z}_V)]$, where Z^S is the capture efficiency of a loop for vacancies or interstitials and $\bar{Z}$ is the average capture efficiency for all other sinks. The continued anisotropy of loop nucleation will generate a corresponding anisotropy in the dislocation network and thus change $\bar{Z}_I$ and $\bar{Z}_V$. This might lead to a reduction of the net bias of a loop as fluence is accumulated. Second, the developing anisotropy of the network is expected to change the intersection probability for loops on the various planes. Since loops unfault to form dislocations with Burgers vectors uniquely suited to unfault other loops of the same Burgers vector,[11] the continued anisotropy of Frank loop nucleation would gradually lead to an increased rate of loop unfaulting on those planes favorably oriented to the applied stresses. In effect the loops would sow the seeds of their own destruction.

CONCLUSIONS

The combined data sets of this and earlier studies clearly show that the SIPA creep mechanism imprints a record of its action in the dislocation and loop microstructures of irradiated metals. The record is not always easily interpretable with respect to the applied stress state, however. The information impressed in the microstructure is easiest to decipher in annealed specimens irradiated to low fluence but significant insight can be gained from cold-worked specimens at low fluence. At higher fluence, the record appears to recede as the loop evolution alters the nature of the other microstructural components which interact and compete with the loops for

the radiation-induced point defects. The greatest difficulty in interpreting the microstructural record arises in those metals which are subject to prolonged high levels of internal stress.

REFERENCES

1. P. R. Okamoto and S. D. Harkness, J. Nucl. Mat., 48, 49 (1973).

2. H. R. Brager, F. A. Garner and G. L.Guthrie, J. Nucl. Mat., 66, 301 (1977).

3. F. A. Garner and W. G. Wolfer, "Microstructural Evidence Supporting the Existence of the SIPA Creep Mechanism," Trans. ANS, San Diego, California (1978), p. 144.

4. F. A. Garner, W. G. Wolfer and H. R. Brager, "A Reassessment of the Role of Stress in Development of Radiation-Induced Microstructure," Proceedings, ASTM 9th International Symposium on Effects of Radiation on Structural Materials, ASTM STP 683, pp. 202-232.

5. W. G. Wolfer, "Correlation of Radiation Creep Theory with Experimental Evidence," University of Wisconsin Report UWFDM-312; also accepted for publication in J. Nucl. Mat.

6. F. A. Garner, E. R. Gilbert and D. Porter, "Stress-Enhanced Swelling of Metals During Irradiation," this conference.

7. M. M. Paxton, B. A. Chin, E. R. Gilbert and R. E. Nygren, J. Nucl. Mat., 80, 144 (1979).

8. H. R. Brager, F. A. Garner, E. R. Gilbert, J. E. Flinn and W. G. Wolfer, "Stress-Affected Microstructural Development and the Creep/Swelling Interrelationship," Radiation Effects in Breeder Reactor Structural Materials, M. L. Bleiberg and J. W. Bennett (Eds), the Metallurgical Society of AIME (1977), pp. 479-507.

9. W. G. Wolfer and M. J. Ashkin, J. Appl. Phys., 46, 547 (1975).

10. W. G. Wolfer, L. K. Mansur and J. A. Sprague, "Theory of Swelling and Irradiation Creep," ibid. Ref. 8, p. 841.

11. D. S. Gelles, "A Frank Loop Unfaulting Mechanism in fcc Metals During Neutron Irradiation," HEDL-SA-2078, Proceedings, International Conference on Dislocation Modeling of Physical Systems, Gainesville, Florida (June 22-27, 1980).